# *Development of a Portable Thermogenerator for Uncontrolled Heat Sources*

**Luis E. Juanicó, Fabián Rinalde, Eduardo Taglialavore & Marcelo Molina**

**Journal of Electronic Materials**

ISSN 0361-5235

Journal of Elec Materi
DOI 10.1007/s11664-012-2449-z

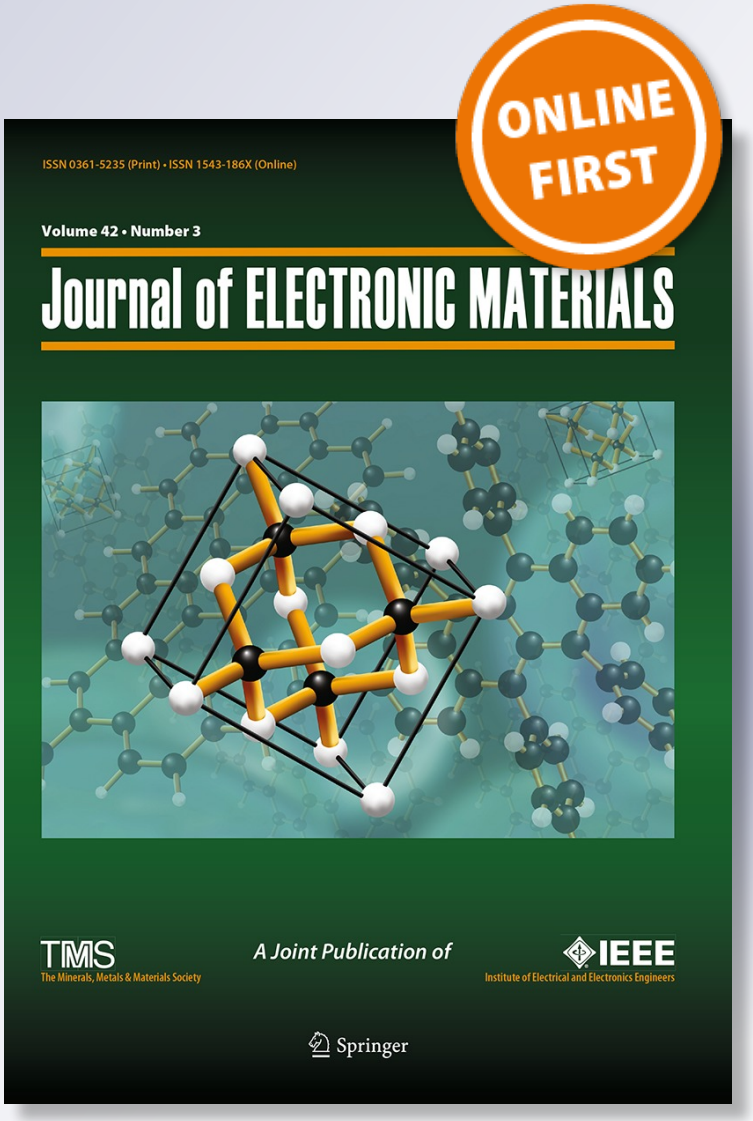


Springer

Journal of ELECTRONIC MATERIALS
DOI: 10.1007/s11664-012-2449-z


# Development of a Portable Thermogenerator for Uncontrolled Heat Sources

LUIS E. JUANICÓ,[1,2] FABIÁN RINALDE,[1] EDUARDO TAGLIALAVORE,[1] and MARCELO MOLINA[1]

1.—National Council of Scientific Research (Conicet) and Balseiro Institute, Bariloche Atomic Center, 8400 Bariloche, Argentina. 2.—e-mail: juanico@cab.cnea.gov.ar

This paper presents the development of a portable thermogenerator designed to work on uncontrolled heat sources. Its thermal behavior regarding both steady-state and transient regimens was analytically described and numerically solved by using a lumped capacity model. The ranges of heating power and power increasing rates have been determined to ensure safe operation, or give users advance warning in case of failure. In addition, this model is a useful tool for designing a controller system based on which a feasible thermogenerator can be developed. Experimental tests performed on a prototype based on a commercial BiTe module have demonstrated this goal.

**Key words:** Thermoelectricity, electrical generator, thermal modeling, numerical simulation, prototype development, lumped capacity thermal model

## INTRODUCTION

Thermoelectric (TE) materials have been known for almost two centuries, although up to now they have not been widely applied for electricity generation except by one company within a single niche market. Global Thermoelectric has sold more than 20,000 generators worldwide for small, isolated applications in the oil and gas industry during the last 40 years,[1] based on a proprietary technology of PbBi TE modules that can withstand up to 600°C. However, these TE modules are not available on the open market, in which only standard Peltier TE modules, operable up to 120°C, have traditionally been the single choice for developers of new applications.[2] However, since this temperature level is too low for most large applications (for example, generators working on firewood stoves for rural homes or generators that work with waste exhaust heat to substitute a car's dynamo), up to now the technology of thermogenerators continues to be largely unknown by the general public.[3]

On the other hand, in recent years TEs have emerged as a feasible option within the portfolio of new sustainable energies,[4–6] due to the irruption of independent manufacturers of BiTe thermogenerator modules such as Tellurex from the USA[7] and Thermonamic from China.[8] Tellurex TEs are priced at 4000 USD/kW, lower than photovoltaic panels, and Thermonamic's are even cheaper at 2500 USD/kW.[2] In addition, during the last 2 years both of these manufacturers have launched new TEs that can withstand up to 320°C. These technological and economic improvements have opened an opportunity window for new niche markets.

This paper presents a new portable generator intended to be used as a small battery charger for recreational use, such as when trekking, mountain climbing, and camping. A prototype was tested, and its thermal transients were analytically modeled and numerically studied including the microcontroller's feedback.

## DEVELOPMENT OF PROTOTYPE

The prototype was developed as two separate (hot and cold) units linked by electrical and signal wires as illustrated in Fig. 1. The hot unit (shown on the left side of Fig. 1) comprises a G1-54-0557 Tellurex module mounted between two aluminum blocks with a fan cooler on top. The hot-side block is a plate

(Received June 8, 2012; accepted December 28, 2012)

Published online: 08 February 2013

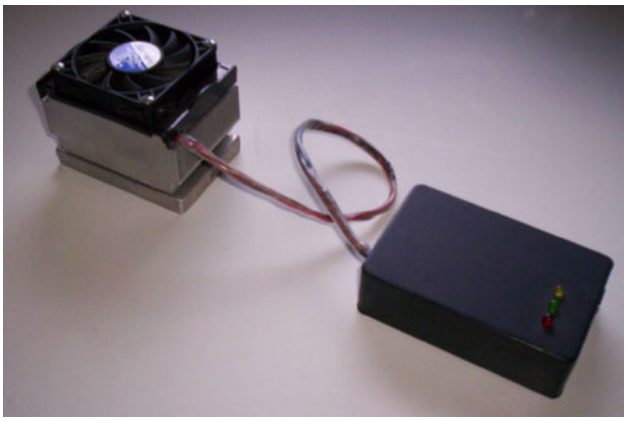

Fig. 1. View of prototype. The left block is the hot unit, and the right block is the cold unit.

(1 cm thick, $6 \times 10^{-3}$ m$^2$ cross section) useful for homogenizing the temperature on the TE's hot side, but since it works on much warmer heating sources than its maximum overheating temperature (175°C), such as firewood or a gas burner, it does not require low thermal resistance. Instead, the cold-side block must minimize its thermal resistance and so is designed to include a finned dissipator cooled by forced air flow. Since the fan is powered just by the thermoelectric generation, it is necessary to have a good thermal–aerodynamic design which matches the characteristics of both the dissipator and fan. Summarizing, this procedure consists of finding the crossing point of the aerodynamic curves (pressure drop versus air flow) of both devices to determine their operation point and hence determine the dissipator thermal resistance and fan power consumption (by using the thermal resistance versus air flow curve of the dissipator and the power versus air flow curve of the fan), which are ultimately the interesting parameters to be optimized. These curves are available data usually provided by manufacturers of standard dissipators and fans in the electronics industry, and this procedure is standard too; a detailed explanation can be found in Ref. 9.

The cold unit comprises all elements that cannot be exposed to high temperatures: (1) the net output power provided by a standard 5-V universal serial bus (USB) port, (2) the analog electronics used for temperature measurement of the TE hot side, (3) the microcontroller, and (4) the user interface built on visual signals [light-emitting diodes (LEDs)] and an audible alarm (piezoelectric buzzer) designed to allow the user to monitor the temperature of the TE's hot side. When the yellow LED is ON, it means that the TE is cold and the hot unit should be moved closer to the fire; conversely, it should be taken away from the fire when the red LED is ON. Finally, the green LED ON means that the temperature is within the optimal operation range. On the other hand, the audible alarm is related to the temperature increasing rate (calculated by the microcontroller) of the TE hot side. The buzzer is activated when the TE is going to achieve its maximum operation temperature (close to the overheating condition) in the next 10 s, and so the user has this warning margin to remove the device from the fire. This warning margin could be extended, for example, by increasing the thermal capacity of both aluminum thermal buffers by increasing their masses. Another control strategy could be setting in advance the fan at its maximum speed when overheating conditions are predicted. All these strategies will be analyzed quantitatively by means of complete thermal modeling performed in the next section.

## THERMAL MODELING

The modeling is performed by using the well-known lumped capacity model[10] in which thermal gradients are neglected inside each subsystem [zero-dimensional (0-D) model] and only transverse heat fluxes across them [one-dimensional (1-D) model] are considered. This combination provides the simplest analytical model but is still suitable for studying stationary and transient processes, in which the whole system can be described as a series of thermal nodes connected by means of thermal resistances as illustrated in Fig. 2. Here, every 0-D node has a homogeneous temperature while there is a temperature drop along every thermal resistance. Although actually thermal gradients cannot be neglected within the thermopile and the dissipator nodes, these challenges are solved by considering two virtual nodes on both sides of the TE module and another one on the dissipator base; in this way, the temperature drops in both the TE module and dissipator can be modeled. In addition, two external nodes are added to introduce the boundary conditions of ambient temperature and heating power.

The TE temperature profile can be calculated for stationary conditions related to the input parameters (thermal resistances) and both boundary conditions of the system. According to Nuwayhid,[11] the contact resistances ($R_{c1}$ and $R_{c2}$) are both equal to 0.1°C/W, and according to the manufacturer, the thermopile resistance is $R_{TE} = 0.6$°C/W.[7] The resistance of the hot-side aluminum plate ($R_1$) can be calculated following this 0-D model as: $R_1 = L/(kA)$, where $L$ and $A$ are the thickness and cross-sectional area, respectively, and $k$ is the aluminum thermal conductivity; hence, $R_1 = 6.28 \times 10^{-3}$°C/W. The dissipator resistance ($R_d$) depends on the fan power and can be characterized by an analytical function fitted from the three-point data commonly supplied by manufacturers; but, considering the starting process in which the fan is switched off, it is necessary to model this condition too. So, the dissipator thermal resistance was calculated by using the well-known heat transfer correlation for parallel channels,[12] and the value $R_d = 2.75$°C/W was obtained.

## Stationary-State Modeling

Using the model of resistances in series, the temperature difference between the two TE sides can be determined and the thermoelectric generation can be calculated based on the TE characterization provided by the manufacturer's data. The results obtained can be parameterized on the heating power as illustrated in Fig. 3 for a 2.3-W fan. This procedure can be repeated for different cooling powers (two steps of 1.3 W and 0.7 W were selected), and the net output power can be calculated as well. These results are summarized in Table I. Here, the noticeable effect of fan consumption related to net power output and to the hot-side TE temperature can be observed. Thus, the net power could be optimized by tuning the cooling power instantly. In addition, the maximum fan power could be set in advance if an increasing rate that will lead to overheating is detected, so that the TE can withstand this process or at least extend the warning period until overheating is reached. All these behaviors were studied, showing that the development of sophisticated control strategies supported by a microcontroller could enhance the thermogenerator performance and margins of safe operation.

On the other hand, it is observed that the device cannot produce any usable power if it is heated slowly (below 45 W). In this case the TE would be steadily warmed up to overheat without starting the fan and without giving any alarm. It is also observed that the existence of a "blind range" for heating powers below 90 W within the thermogenerator cannot produce enough energy to support the minimum cooling level (0.7 W), and this could lead to overheating without ever starting the fan. Thus, it is also necessary to analyze the transient starting process.

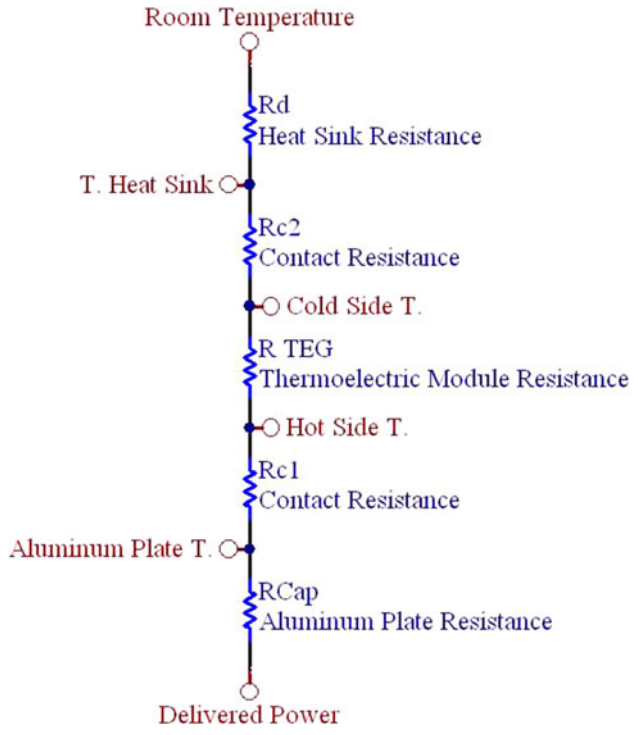


Fig. 2. Scheme of thermal resistances in series.

## Dynamic Modeling of the Starting Transient

The previous lumped capacity model was used again to model the thermal dynamics. Its main hypothesis implies a homogeneous temperature inside each capacitance node, which is a good approximation for four nodes of this system: both thin ceramic buffers (around both sides of the TE) and the heat collector and dissipator base. Here, for example, the thermal gradient along the heat collector can be estimated according to Fourier's law for heat conduction as $q'' = (\Delta T k)/t$. So, in order to transfer 150 W (on $6 \times 10^{-3}$ m$^2$, this implies a heat flux of $q'' = 25 \times 10^3$ W/m$^2$) through a 1 cm thickness ($t$), a small temperature drop is obtained ($\Delta T = 1$°C), negligible in comparison with the full temperature drop (of about 150°C). However, the fifth node of this model represents the $Bi_2Te_3$ thermopile itself, in which the thermal gradient cannot be neglected. So, this node implies a major challenge for developing a simple analytical model, which will be solved by adding other thermal approximations. Let us remark that complex models commonly used in engineering [such as three-dimensional (3-D) finite-element models] require very large computational resources that are outside the scope of a conceptual design tool. The five-node model represents the thermal dynamics of the system by means of the energy balance of each node as shown in Eqs. (1–5):

$$M_{\mathrm{HC}} Cp_{\mathrm{Al}} \frac{\mathrm{dT_{HC}}}{\mathrm{d}t} = q_0(t) - \frac{T_{\mathrm{HC}} - T_{\mathrm{hot}}}{R_{C1}}, \quad (1)$$

$$M_{\mathrm{Cer}} Cp_{\mathrm{Cer}} \frac{\mathrm{dT_{hot}}}{\mathrm{d}t} = \frac{T_{\mathrm{HC}} - T_{\mathrm{hot}}}{R_{C1}} - \frac{T_{\mathrm{hot}} - T_{\mathrm{TE}}}{R_{\mathrm{TE}}/2}, \quad (2)$$

$$M_{\mathrm{TE}} Cp_{\mathrm{TE}} \frac{\mathrm{dT_{TE}}}{\mathrm{d}t} = \frac{T_{\mathrm{hot}} - T_{\mathrm{TE}}}{R_{\mathrm{TE}}/2} - \frac{T_{\mathrm{TE}} - T_{\mathrm{cold}}}{R_{\mathrm{TE}}/2}, \quad (3)$$

$$M_{\mathrm{Cer}} Cp_{\mathrm{Cer}} \frac{\mathrm{dT_{cold}}}{\mathrm{d}t} = \frac{T_{\mathrm{TE}} - T_{\mathrm{cold}}}{R_{\mathrm{TE}}/2} - \frac{T_{\mathrm{cold}} - T_{\mathrm{dis}}}{R_{C2}}, \quad (4)$$

$$M_{\mathrm{dis}} Cp_{\mathrm{Al}} \frac{\mathrm{dT_{dis}}}{\mathrm{d}t} = \frac{T_{\mathrm{cold}} - T_{\mathrm{dis}}}{R_{C2}} - \frac{T_{\mathrm{dis}} - T_{\mathrm{amb}}}{R_{\mathrm{dis}}}, \quad (5)$$

where $M_{\mathrm{HC}}$, $M_{\mathrm{dis}}$, $M_{\mathrm{Cer}}$, and $M_{\mathrm{TE}}$ are the masses of the heat collector, dissipator, ceramic buffer, and

thermoelectric, respectively; $Cp_{Al}$ is the aluminum heat capacity, $q_0(t)$ is the instant heat power supplied, and $T_{HC}$, $T_{hot}$, $T_{cold}$, $T_{dis}$, and $T_{amb}$ are the temperatures of the heat collector, both sides of the TE, the dissipator, and the ambient air, respectively. Here, and considering aluminum blocks of relative large size, this model can be simplified by neglecting the *thermal inertia* of both ceramic buffers and thermoelectric nodes, this being the last key to avoid the challenge previously mentioned. The thermal inertia of any block can be represented by the product of its mass and heat capacity, shown in Table II, here; it is observed that the previous assumption is reasonable. On this hypothesis the left terms of Eqs. 2–4 can be neglected. Thus, it can be demonstrated that the thermoelectric node equation (Eq. 3) can be eliminated if the thermoelectric temperature $T_{TE}$ is approximated in every moment as well as the average of both sides, that is: $T_{TE} = (T_H + T_C)/2$. Let us note that this approximation is exact in the stationary condition, in which a linear temperature profile along the thermoelectric material is obtained. Using this assumption, the model can be rewritten as the following four-equation system (6–9):

$$M_{HC} Cp_{Al} \frac{dT_{HC}}{dt} = q_0(t) - \frac{T_{HC} - T_{hot}}{R_{C1}}, \tag{6}$$

$$\frac{T_{HC} - T_{hot}}{R_{C1}} = \frac{T_{cold} - T_{dis}}{R_{C2},} \tag{7}$$

$$\frac{T_{cold} - T_{dis}}{R_{C2}} = \frac{T_{hot} - T_{cold}}{R_{TE},} \tag{8}$$

$$M_{dis} Cp_{Al} \frac{dT_{dis}}{dt} = \frac{T_{cold} - T_{dis}}{R_{C2}} - \frac{T_{dis} - T_{amb}}{R_{dis}}. \tag{9}$$

## Numerical Simulation of Transients

The previous four-equation system was solved numerically for different thermal transients related to steps and linear increasing rates of heating power

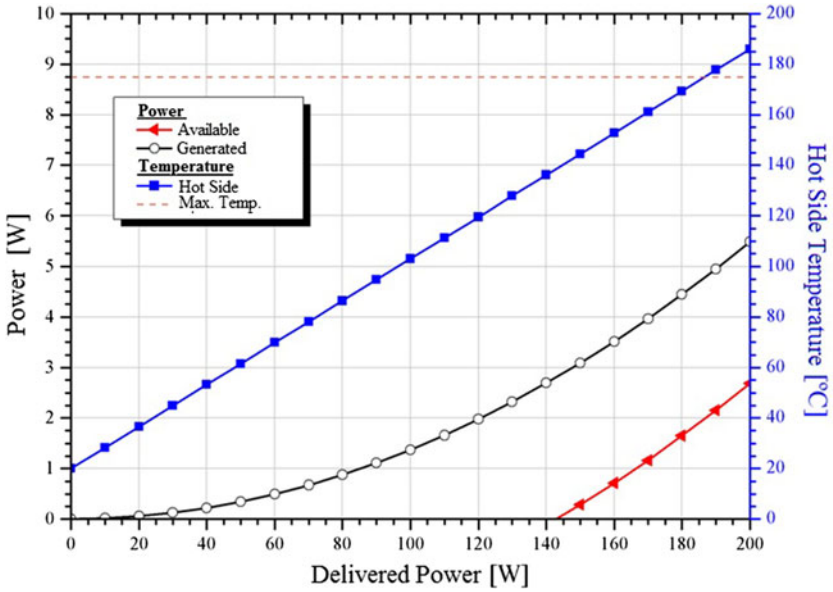


Fig. 3. Stationary process for 2.3-W fan power.

**Table I. Results for different fan powers**

| Fan Power (W) | Max. Net Output (W) | Min. Heating Power (W) | Max. Heating Power (W) |
|---|---|---|---|
| 2.3 | 2.2 | 140 | 190 |
| 1.3 | 2.5 | 115 | 175 |
| 0.7 | 2.0 | 90 | 150 |
| Off | – | – | – |

Maximum and minimum heating power relate to maximum TE temperature and zero net output, respectively.

**Table II. The relative thermal inertia of every node**

| Subsystem | Mass (kg) | Heat Capacity (J kg/m°C) | $M \times C_p$ | Relative Weight (%) |
|---|---|---|---|---|
| Heat collector | 0.18 | 903 | 162.5 | 28.1 |
| Ceramic buffer | $5 \times 10^{-3}$ | 500 | 2.5 | 0.4 |
| Thermopile | 0.04 | 170 | 6.8 | 1.2 |
| Dissipator | 0.45 | 903 | 406.4 | 70 |

**Table III. Table of heating power ranges for safe operation**

| | |
|---|---|
| Maximum power without fan and without alarms | 45 W |
| Minimum power without fan and with alarms | 75 W |
| Minimum power with fan on (0.7 W) | 100 W |
| Maximum power with fan on (1.4 W) | 175 W |
| Maximum power with fan on (2.3 W) | 185 W |
| Maximum power for 10-s warning | 1000 W |

by using the numerical MATLAB/Simulink framework. In every case, the numerical stability of the solution was checked, the relative local error set lower than $10^{-7}$, and the numerical scheme selected was (ODE45) Runge–Kutta. The objectives of this study are: (1) to determine the system's characteristic response time, and (2) to determine the range of power within which the system can be safety operated, both parameters being key to design the control strategy.

*Transient Evolution for Power Steps*

Here the system response under starting power steps is studied; For example, these are cases in which the "cold" TE is immediately put onto the heat source. Different initial power steps are studied under different cooling powers to determine the ranges of operation. Table III summarizes these results. Here, we observe the existence of a "blind range" between 45 W and 75 W in which the system cannot power its electronic system (that is, the TE generates less than 0.7 W) before reaching the maximum TE temperature (175°C). Above this range, there is another range of risk (up to 100 W) in which the generation is sufficient to power the alarm system but not to start the fan as well. Above this level the fan can be started before the TE overheats and so the TE temperatures are dramatically reduced, which in turn leads to greater TE generation and greater cooling flow following a positive feedback process. Therefore, there is a safety range between 100 W and 185 W within which the device can be self-controlled. Higher heating power leads to an overheating condition, but the device can activate the alarms in advance. The minimum warning time (10 s) is achieved for heating power of 1000 W, which represents a huge 166 kW/m$^2$ flux that is not a realistic value.

*Transient Evolution for Linearly Increasing Rates of Power*

Different increasing rates of heating power for the starting process were studied to determine the ranges for safe operation. Table IV summarizes the results for the maximum and minimum power rates in which the 10-s warning is achieved. The temporal evolution of the TE temperatures and power generation for the maximum power rate is illustrated in Figs. 4 and 5, respectively. Here, it is observed that the TE reaches its maximum temperature (175°C) at 18.5 s, while the generation threshold for powering the electronic system (0.7 W) is reached in 8.5 s. Similar to the previous case analyzed for power steps, this maximum level is so high (and conversely the minimum rate so low) that it does not represent a realistic condition.

*Transient Evolution with Controlling System*

It has been observed that the cooling flow has a noticeable effect on the TE's performance; for example, when setting a higher fan power, the thermoelectric generation is increased beyond the added consumption. However, this behavior should be checked regarding a realistic starting process in which the TE temperature drop is progressively increased and a higher cooling power is accordingly set. This feature is performed by including a controlling loop (made as a new block in the Simulink framework) that changes the dissipator resistance as a function of the fan power, which in turn is set according to the TE generation available.

Figures 6 and 7 show the power parameters and temperature evolutions, respectively, for the starting process for 185 W of heating power. It starts on free convection cooling, and after 150 s the controlling system detects that the TE generation reaches 1.4 W (needed to power the electronic system and the fan) and starts the fan at its lower level. This action causes a noticeable effect, immediately decreasing the net output, but after that the dissipator temperature decreases steadily and so the net output increases. After 280 s the controlling system

sets the fan to 1.3 W, after which the system evolves asymptotically to a steady-state condition providing net output of 2.4 W.

**Table IV. Ranges of heating power rates for starting process**

| | |
|---|---|
| Maximum rate with 10-s warning | 180 W/s |
| Minimum rate with 10-s warning | 0.03 W/s |

## EXPERIMENTAL VALIDATION

The built prototype was tested to validate the thermal modeling. An experimental setup was constructed by an electrical heater and standard temperature and electrical sensors to measure all the variables. The heating power was not directly measured (nor was the thermogenerator thermally isolated, a very cumbersome task), but rather the TE itself was used as a power sensor by using the

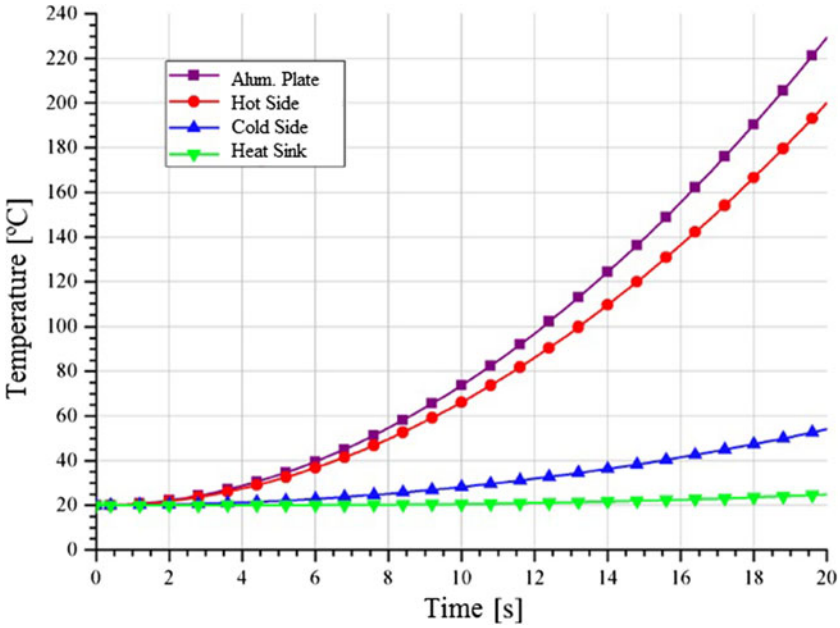


Fig. 4. Evolution of TE temperatures for heating rate of 180 W/s.

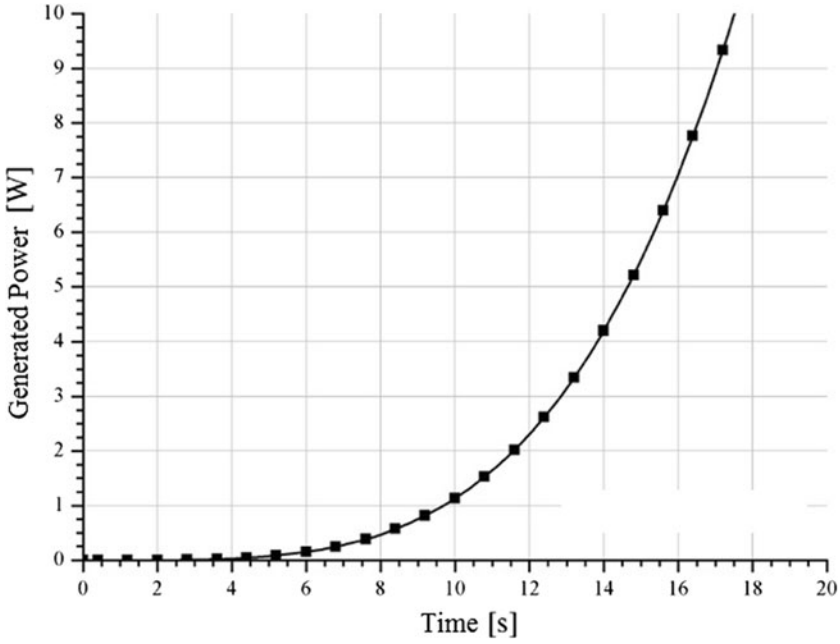


Fig. 5. Evolution of TE generation for heating rate of 180 W/s.

manufacturer's data and the temperature measurements at each node.

Figure 8 shows the experimental and simulated evolution for a starting process with 100 W of heating power and maximum fan power (2.3 W), in which good agreement within the experimental (±5%) errors is observed. Similar behaviors were observed for other cases within the safe operation range.

After having performed these tests without a controlling system, the transient process was verified including this system. Therefore, a 170-W test was performed, including the microcontroller developed (the cold unit) in this prototype. The evolution is illustrated in Fig. 9, showing good agreement with the numerical simulation, thus the validation also applied to the dynamics of fan cooling.

## CONCLUSIONS

Complete thermal modeling for a thermogenerator was developed. This is useful to study the

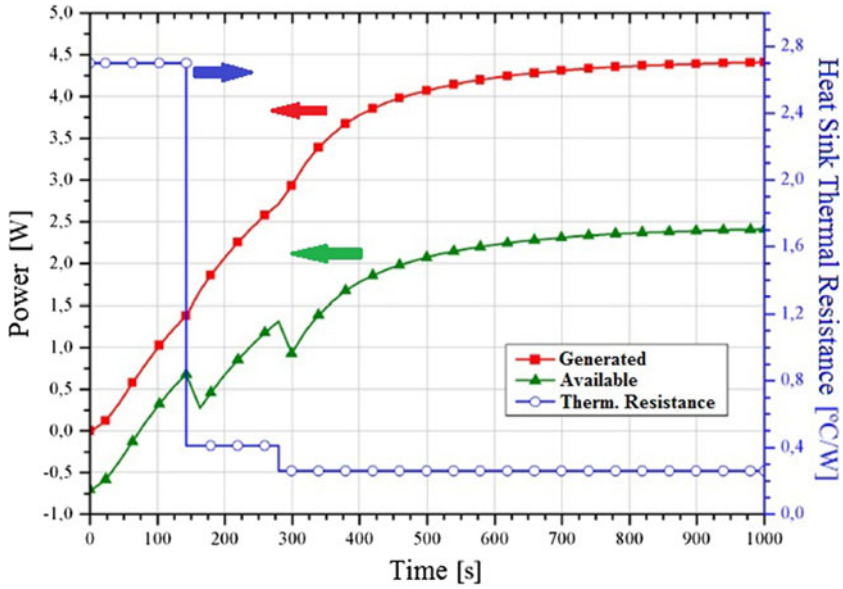


Fig. 6. Evolution of powers for 185 W of heating power.

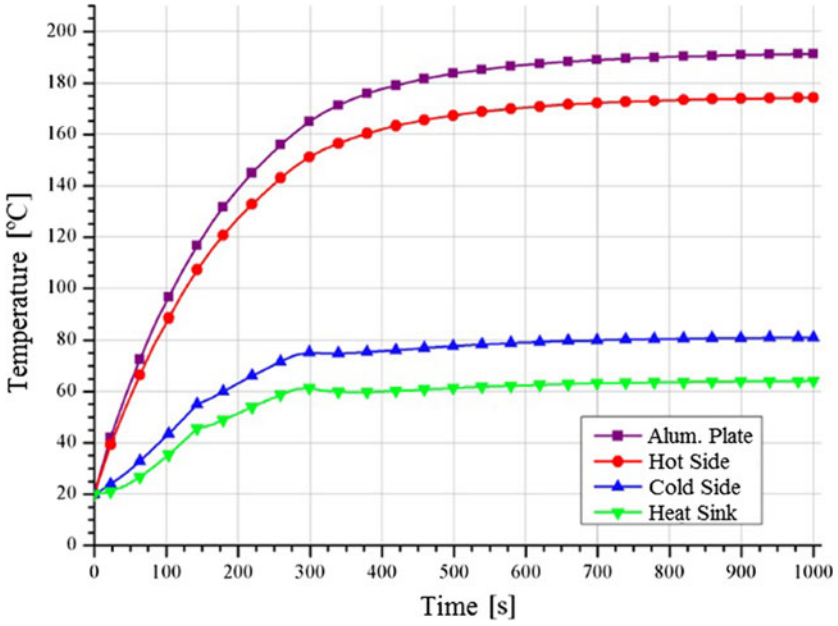


Fig. 7. Evolution of temperatures for 185 W of heating power.

intrinsically linked mechanisms of thermoelectric generation and thermal transfer. Although this model is based on the simplest 0-D lumped capacity model, it is suitable for studying stationary and transient processes, as was experimentally verified. Moreover, it is a useful design tool for the controlling system, a key feature in obtaining a feasible thermogenerator working on uncontrolled heat sources.

The choice of a self-powered cooling system implies a major challenge for the controller, solved by the user monitoring system. However, there is a "blind range" (between 45 W and 75 W) in which the TE overheats without warning or activating the fan. This could be solved by adding a battery that energizes the electronic system during the starting process, or redesigning the electronic system so that it can work on a lower voltage threshold.

On the other hand, a different approach to solve the previous problem can be obtained through the thermal design. The TE temperature drop would be increased during the starting transient by increasing the dissipator mass and decreasing the heat collector mass. In this way, the thermal inertia of both elements is

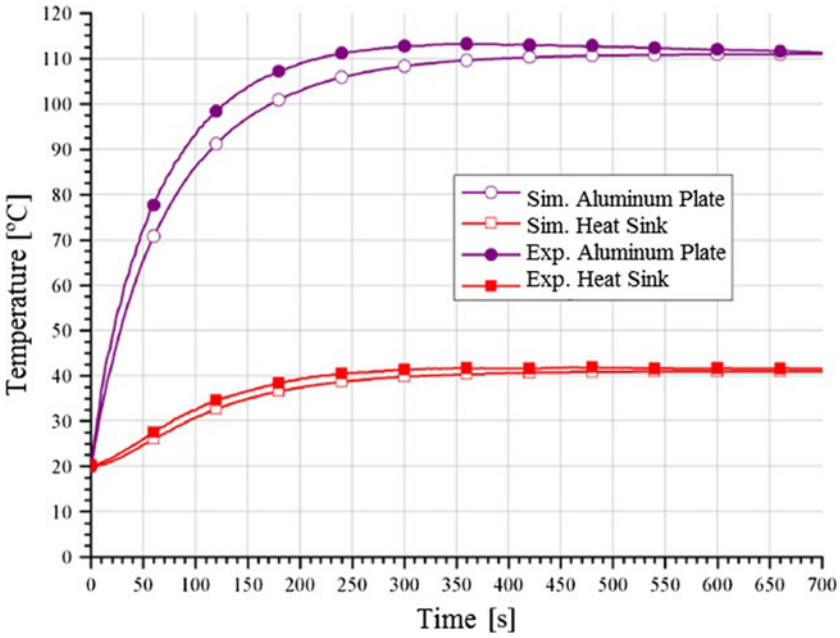


Fig. 8. Experimental and simulated evolutions for 100 W step.

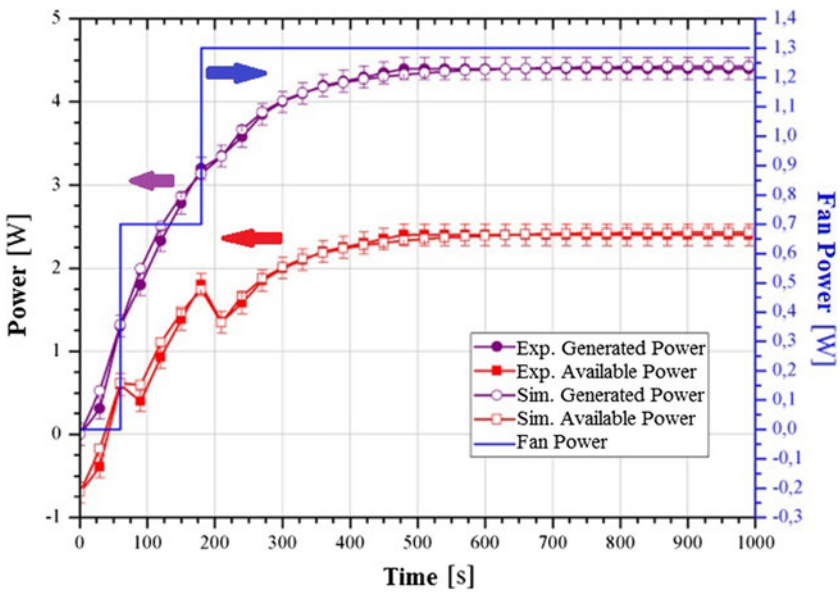


Fig. 9. Experimental and simulated evolutions for 170 W step with controlling system.

modified conveniently, increasing the heat collector temperature and decreasing the dissipator temperature, considering that both TE hot and cold sides follow the heat collector and dissipator temperatures, respectively. This and other trends can be better studied by means of an analytical tool such as this model. Furthermore, such an analytical tool allows us to change the TE parameters easily to study other kinds of thermopiles. In particular, the recently launched TE that can withstand up to 350°C provides a much better solution for concerns about TE overheating, besides providing higher powers with a smaller dissipator and even eliminating the fan consumption. They will clearly be the next step in thermoelectricity applications.

## REFERENCES


1. E.M. Petrie, *Distributed Generation from Baseload to Backyard, Chap. 20* (PennWell: International Electric Power Encyclopedia, 1999).
2. R. Buist and P. Lau, *Thermoelectric Power Design and Selection from TE Cooling Module Specifications, 16th Int Conference on Thermoelectrics* (Dresden, Germany, 1997), pp. 551–554.
3. L. Juanicó and F. Rinalde, *J. Renew. Sustain. Energy* 1, 043107 (2009).
4. H.J. Goldsmid, *Introduction to Thermoelectricity* (New York: Springer, 2009).
5. S. Maneewan, J. Khedari, B. Zeghmati, J. Hirunlabh, and J. Eakburanawat, *Renew. Energy* 29, 743 (2004).
6. Z.H. Dughaish, *Phys. B* 322, 205 (2002).
7. See Web Site of Tellurex, http://www.tellurex.com. Accessed 21 December 2012.
8. See web Site of Thermonamic, http://www.thermonamic.com/. Accessed 21 December 2012.
9. D. Mastbergen, B. Willson, and S. Joshi. Producing Light from Stoves Using a Thermoelectric Generator. http://bioenergylists.org/stovesdoc/ethos/mastbergen/Mastbergen_ETHOS_2005.pdf. Accessed 21 December 2012.
10. F. Incropera and D. DeWitt, *Fundamentals of Heat and Mass Transfer*, 6th ed. (New Jersey: Wiley, 2007).
11. R. Nuwayhid, D. Rowe, and G. Min, *Renew. Energy* 28, 205 (2003).
12. A. Bar-Cohen and W. Rohsenow, *J. Heat Transf.* 106, 116 (1984).